Integration of TES Microcalorimeters With Microwave SQUID Multiplexed Readout

Douglas A. Bennett, John A. B. Mates, Johnathon D. Gard, Andrew S. Hoover, Michael W. Rabin, Carl D. Reintsema, Daniel R. Schmidt, Leila R. Vale, and Joel N. Ullom

***Abstract*—The demonstration of a microwave superconducting quantum interference device (SQUID) multiplexed readout of transition-edge sensor (TES) microcalorimeters has the potential to dramatically expand the scale of arrays of TESs. In this paper, we discuss recent work to develop an instrument for high-resolution high-efficiency gamma-ray spectroscopy that integrates previously demonstrated high-resolution TES microcalorimeters with new lower noise microwave SQUID multiplexers. We will discuss the proposed instrument design and readout noise of the optimized microwave SQUID multiplexed readout. Finally, we will discuss the potential limits on the number of multiplexed TESs imposed by the analog-to-digital converter.**

***Index Terms*—SQUIDs, superconducting microwave devices, superconducting photodectectors.**

I. Introduction

HIGH-RESOLUTION gamma-ray spectroscopy using arrays of transition-edge sensor (TES) microcalorimeters has been previously demonstrated using the NIST-LANL microcalorimeter array [1], [2]. This instrument utilizes a time-division multiplexed (TDM) readout. Currently TDM is the most mature of the TES multiplexing schemes having demonstrated 256 calorimeters in an 8 by 32 format [1] and 10,240 TES bolometers in 8 units of 32 by 40 [3]. However, increasing the multiplexing factor much beyond 32–40 sensors is difficult due to the multiplexing penalty inherent in TDM that scales as the square root of the number of rows [4]. Recently an alternate multiplexing scheme, microwave SQUID multiplexing [5], demonstrated successful simultaneous readout of two TES microcalorimeters with $E/\Delta E > 1000$ [6]. Microwave SQUID multiplexing does not have the multiplexing penalty that is an issue with TDM, and is able to take advantage of the significantly larger bandwidth that is possible at microwave frequencies. In this paper, we describe recent work towards developing a new gamma-ray spectrometer that is a pathfinder instrument that integrates high-resolution TES microcalorimeters, new lower noise microwave SQUID multiplexing chips, and array compatible microwave electronics. Finally we compute the limits that the analog to digital converter (ADC) will impose on the number of pixels that can be read out per ADC.

In the context of this paper, a microwave SQUID multiplexer (μMUX) element [7], [8] consists of a dissipationless RF SQUID that is coupled to a microwave resonator such that a change in the inductance of the SQUID shifts the resonant frequency of the resonator. Many resonators, each with a unique resonant frequency, are coupled to a common feed line. Each resonator, and therefore each SQUID, can be addressed simultaneously by using a comb of probing frequencies. The responses of all the RF SQUIDs can be linearized by applying a single flux ramp modulation to all SQUIDs [9]. After digitization, the resonator response signal can be demodulated in firmware or software to reproduce the input signal of the SQUID. The flux ramp modulation has the added benefit of modulating the signal from the TES to higher frequencies, avoiding much of the two-level noise that gives a strong $1/f^{1/2}$ dependence to the noise observed in superconducting resonators. A detailed description of the μMUX designs can be found in Ref. [8].

II. Sledgehammer

The prototype μMUX based spectrometer is known as the **S**pectrometer to **L**everage **E**xtensive **D**evelopment of **G**amma-ray T**E**Ss for **H**uge **A**rrays using **M**icrowave **M**ultiplexed **E**nabled **R**eadout or **SLEDGEHAMMER**. It will consist of 256 TES microcalorimeters read out by eight μMUX chips of 32 channels each. The first version has the eight μMUX chips separated into four different frequency bands. The entire array is read out on four coaxial cables, two for the input microwave tones and two for the output tones. The layout of the sample box with the necessary chips is shown in Fig. 1. There are also eight interface chips that contain the shunt resistors and Nyquist inductors necessary for optimum TES operation. Finally, there are additional adapter chips that will allow flexible signal routing to match the linear layout of the μMUX chips to the close-packed array format of the TESs. The gamma-rays enter the box through a hole in the lid of the box above the detectors (lid not shown).

The microwave signals are brought into the sample box using the 4 SMA connectors at the four corners of the box. The microwave launches between the SMA connectors and μMUX chips are currently being optimized to reduce standing

Manuscript received August 12, 2014; accepted December 1, 2014. Date of publication December 22, 2014; date of current version February 6, 2015. This work was supported in part by the DOE NEUP program under Grant DE-NE0000716001, by the NIST Innovations in Measurement Science Program, and by the NASA APRA program.

D. A. Bennett, J. A. B. Mates, C. D. Reintsema, and L. R. Vale are with the Quantum Electronics and Photonics Division, National Institute of Standards and Technology, Boulder, CO 80305 USA (e-mail: douglas.bennett@nist.gov).

J. D. Gard, D. R. Schmidt, and J. N. Ullom are with the National Institute of Standards and Technology, Boulder, CO 80305 USA, and also with the University of Colorado Boulder, Boulder, CO 80309-0399 USA.

A. S. Hoover and M. W. Rabin are with the Los Alamos National Laboratory, Los Alamos, NM 87545 USA.

Color versions of one or more of the figures in this paper are available online at http://ieeexplore.ieee.org.

Digital Object Identifier 10.1109/TASC.2014.2381878

1051-8223 © 2014 IEEE. Personal use is permitted, but republication/redistribution requires IEEE permission.
See http://www.ieee.org/publications_standards/publications/rights/index.html for more information.

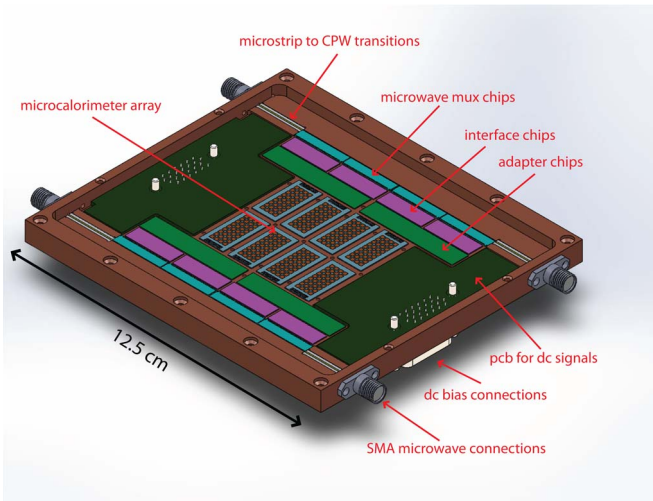

Fig. 1. Drawing of the sample box and chip layout for the SLEDGEHAMMER instrument. The 256 gamma-ray TES microcalorimeters are on the eight chips located in the middle box. The 8 μMUX chips complete the transmission line path at the top right and bottom left of the sketch.

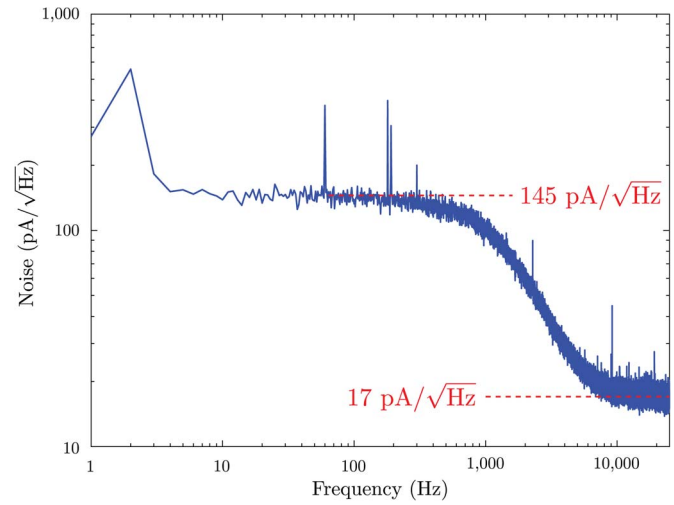

Fig. 2. Measured current noise of gamma-ray TES microcalorimeters read out with a microwave SQUID multiplexer with flux ramp modulation. The detector noise rolls off above approximately 1 kHz and reaches the noise floor of the readout at 17 pA/Hz$^{1/2}$ at 10 kHz.

waves across the inside of the box. The current design uses a microstrip to coplanar waveguide (CPW) transition on a microwave compatible substrate. The μMUX chips are separated into banks of four, where each of the four chips is a separate band. If it is possible to achieve eight bands of 32 resonators within the bandwidth of the readout chain, then the output of one bank can be connected to the input of the other with a coaxial cable. The TES bias, the flux ramp signals, and other low frequency diagnostic wiring enter the sample box by the two 25 pin connectors and are routed using pc boards at both ends of the sample box.

The SLEDGEHAMMER sample box will be mounted on the cold stage of a single stage adiabatic demagnetization refrigerator (ADR) backed by a sorption-pumped ^{3}He stage. This ADR should be capable of cooling the sample box and the necessary coaxial cables to 80 mK and holding for a few days before it will be necessary to cycle the ADR and regenerate the ^{3}He. The sample box will be protected from both the ADR magnet and magnetic fields in the laboratory by high permeability and superconducting shields.

The design of the μMUX chips are described elsewhere [8]. A major design change compared to the μMUX devices in a previous gamma-ray TES demonstration [6] was to increase the input coupling to improve the gain. With this higher gain, the TES noise is significantly above the noise contribution the high-electron-mobility transistor (HEMT). The achieved readout noise referred to the SQUID input in the previous design was 86 pA/Hz$^{1/2}$. In the new design, the increased input coupling (232 pH) has improved the readout noise to 17 pA/Hz$^{1/2}$, well below the in-band TES noise of 145 pA/Hz$^{1/2}$, see Fig. 2.

This readout noise is consistent with the $\approx$3 K noise temperature of the HEMT. The voltage at the HEMT input referred to the SQUID input, or trans-impedance gain, of the μMUX is [8]

$$\frac{dV}{dI} = \omega_0 p \pi M_{in} \sqrt{\eta} \sqrt{\frac{Z_0}{2\omega_0 L_J}} \tag{1}$$

where Z_0 is the impedance of the feed line, ω_0 is the resonance frequency, M_{in} is the input inductance of the SQUID, and L_J is the Josephson inductance of the SQUID. p is the peak-to-peak flux amplitude in the SQUID in units of Φ_0 [8]

$$p \equiv \frac{\Delta\Phi_{p-p}}{\Phi_0} = V_{in} \frac{4M_c}{\Phi_0 Z_0} \sqrt{\frac{2Q_c Z_0}{\pi Z_1}} \tag{2}$$

where M_c is the mutual inductance between the SQUID and the resonator, Z_1 is the characteristic impedance of the resonator, and Q_c is the coupled Q of the resonator set by the coupling capacitance to the feed line. η is the SQUID to resonator coupling strength defined as the change in frequency over the bandwidth of the resonator.

$$\eta \equiv \frac{\Delta f_{p-p}}{\mathrm{BW}} = \frac{4\omega_0 Q_c M_c^2}{\Phi_0 Z_1 L_s} \frac{\lambda}{1-\lambda^2} \tag{3}$$

where $\lambda = L_s/L_J$, and L_s is the self inductance of the SQUID. The voltage noise of the HEMT is $S_V = 4k_B T_N Z_0$ where T_N is the noise temperature of the HEMT. If we use the design parameters $\eta \approx 1/2$ and $p = 2/\pi$, $L_J = 60$ pH, $M_{in} = 232$ pH, $\omega_0 = 5$ GHz, $Z_0 = 50\ \Omega$ and assume a noise temperature for the HEMT of 3 K, then the current noise referred to the input of the SQUID is 5 pA/Hz$^{1/2}$, or 7 pA/Hz$^{1/2}$ with the flux ramp penalty. This does not include any contributions from two-level system noise or from masking out some of the signal during the flux ramp reset. Taking this into consideration, the prediction is roughly consistent with the measured noise (Fig. 2). This improved readout noise floor will allow ample margin to read out the SLEDGEHAMMER gamma-ray TESs without degrading energy resolution.

The readout electronics, both hardware and firmware, are an extension of the open source microwave electronics developed by the MUSIC [10], [11] and ARCONS [12] collaborations for the read out of MKID arrays. The hardware and firmware tools were developed within the Reconfigurable Open Architecture Computing Hardware (ROACH) platform that was developed

and is maintained by the CASPER Collaboration [13]. The initial electronics for SLEDGEHAMMER will use the ROACH2 (based on Xilinx Virtex-6 FPGA) and the MUSIC ADC/DAC board (2 channel, 550 MSPS, 12-bit ADC and 2 channel, 1000 MSPS, 16-bit DAC). The microwave electronics generate the necessary tones to probe the resonators at baseband, mix this signal up to the microwave range to interrogate the phase shift in the resonators, mix down to baseband, digitize the signal with a fast ADC, and then separate the signals in firmware. For SLEDGEHAMMER, it is necessary to augment the ARCONS firmware with the ability to demodulate the flux ramp modulation.

SLEDGEHAMMER is a path finder instrument that will be used to help understand the scalability limits imposed by the μMUX readout and the microwave electronics. As the microwave electronics are improved, it is assumed that the bandwidth of the cryogenic HEMT will ultimately limit the total number of pixels that can be read out per μMUX chain. However, each portion of the readout chain must be studied in order to demonstrate the necessary scalability to meet the future needs for kilo-pixel and eventually mega-pixel arrays of TES microcalorimeters. In this paper we will further explore the requirements for one component of the readout, the noise due to the digitization of the signal by the analog-to-digital converter (ADC).

III. Limits Imposed by Digitization

One potential concern for the μMUX readout is the limitation imposed by the ADC measuring the baseband signals. For an ADC with b bits and sampling at f_s, the maximum error for an ideal ADC is given by the least significant bit (LSB) as $\pm(1/2)LSB$. The error in an AC signal that spans more than a few LSBs can be approximated as a sawtooth waveform with a peak-to-peak amplitude equal to 1 LSB (q). The equation of the sawtooth error is $e(t) = st$ from $-q/2s < t < +q/2s$ where s is the slope of the sawtooth [14]. Integrating to find the root-mean-square value gives

$$\sqrt{\overline{e^2(t)}} = \frac{q}{\sqrt{12}}. \tag{4}$$

The quantization error is approximately Gaussian and approximately spread over the entire bandwidth from dc to $f_s/2$. Assuming the input to the ADC is a full scale sine wave

$$v(t) = \frac{q2^b}{2}\sin(2\pi f t) \tag{5}$$

then the RMS value is

$$\sqrt{\overline{v^2(t)}} = \frac{q2^b}{2\sqrt{2}}. \tag{6}$$

Combining (4) and (6) and using dB, we have the classic equation for the signal-to-noise ratio (SNR) from quantization in an ADC [14]

$$\text{SNR} = 20\log_{10}\left[\frac{q2^b/2\sqrt{2}}{q/\sqrt{12}}\right] = 6.02b + 1.76\ \text{dB} \tag{7}$$

over the range from dc to the Nyquist bandwidth ($f_s/2$).

However, this SNR can be improved when the signal that is being measured occupies a smaller bandwidth (BW) and the signal is therefore oversampled. As long as an ideal digital filter is used to filter out the noise components outside of the bandwidth, there is a correction factor [15] to (7)

$$\text{SNR} = 6.02b + 1.76 + 10\log_{10}\left(\frac{f_s}{2\times\text{BW}}\right) \tag{8}$$

over the bandwidth of the measurement BW.

If instead of a sine wave, the power is Gaussian distributed and the signal is scaled such that the full range of the ADC, $\pm A_{clip}$, is some multiple of the total RMS power, $\mu = A_{clip}/\sigma$, the SNR becomes

$$\text{SNR} = 10\log_{10}\left[\frac{\sigma^2/A_{clip}^2}{q^2/12}\right] = 10\log_{10}\left[\frac{3*2^{2b}}{\mu^2}\right] \tag{9}$$

$$\text{SNR} = 6.02b - 20\log_{10}(\mu) + 4.77\ \text{dB}. \tag{10}$$

There is an additional noise term related to the clipping of the signal when all the tones are summed. Therefore, there is a tradeoff between using a larger signal to reduce the quantization noise and using a smaller signal to reduce the noise due to clipping the signal on the full range of the ADC.

The output signal of the μMUX consists of N readout tones summed together with the TES response encoded in the phase. This is a common occurrence for multi-tone communications systems, i.e., multi-carrier Quadrature Amplitude Modulation (QAM). These multi-tone signals are often quantified by their peak to average power ratio

$$PAPR = \lim_{T\to\infty}\frac{\max|v(t)|^2}{\frac{1}{T}\int_0^T v^2(t)\,dt} \tag{11}$$

for a signal $v(t)$. The crest factor is related to the PAPR as $CF = \sqrt{PAPR}$. The CF for a normalized square wave is 1 since its RMS amplitude is equal to its magnitude. For a normalized sine wave the $CF = \sqrt{2}$. The CF for a multi-carrier signal initially grows rapidly with N, but for random phases at $N = 10$ the signal power in the tails of the distribution is reasonably well approximated by a Gaussian probability density function as described by the central limit theorem [16]. By around $N = 16$, the Gaussian approximation to the power in the tails is very good. The Gaussian probability density function is the limit $N \to \infty$, so the tails of any finite N will be smaller.

In order to compare to the quantization noise, we need to quantify the distortion due to clipping the combined signal. Assuming a Gaussian probability distribution, the signal $v(t)$ takes the value x with a zero mean and a variance σ^2

$$p(x) = \frac{1}{\sigma\sqrt{2\pi}}e^{-\frac{x^2}{2\sigma^2}}. \tag{12}$$

The total power of the clipped portion [17] is

$$P_{clip} = 2\int_{A_{clip}}^{\infty}(x - A_{clip})^2 p(x)\,dx \tag{13}$$

$$P_{clip} = \sigma^2\left[(1+\mu^2)\,\text{erfc}\left(\frac{\mu}{\sqrt{2}}\right) - \sqrt{\frac{2}{\pi}}\mu e^{\frac{-\mu^2}{2}}\right] \tag{14}$$

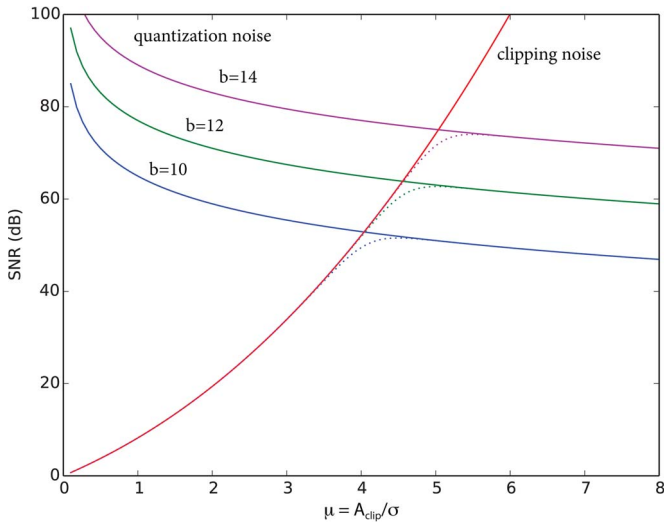

Fig. 3. Signal-to-noise ratio for the clipping noise (red) and the quantization noise of a Gaussian signal for 10 bits (blue), 12 bits (green), and 14 bits (magenta). The combined SNRs of the quantization and clipping are shown by the dotted lines.

and therefore the SNR (not in dB) due to clipping is

$$\mathrm{SNR}_{clip} = \left[(1+\mu^2)\,\mathrm{erfc}\left(\frac{\mu}{\sqrt{2}}\right) - \sqrt{\frac{2}{\pi}}\mu e^{\frac{-\mu^2}{2}}\right]^{-1}. \quad (15)$$

In Fig. 3, the SNR due to clipping noise (15) is compared to the SNR for quantization noise (9) as a function of μ. As μ is increased, less of the signal is clipped, so the SNR of the clipping noise goes up. However this causes most of the signal to be spread over fewer bits so the SNR of the quantization noise goes down. For a given number of bits, there is an optimal value of μ, e.g., for $b = 10$ $\mu = 4.5$, for $b = 12$ $\mu = 5.0$, and for $b = 14$ $\mu = 5.5$. Also, at the optimum μ, the SNR of the quantization noise is a good approximation for the SNRs added in quadrature.

The single-tone SNR of a multi-tone signal is

$$\mathrm{SNR} = 6.02b - 10\log_{10}(N) - 20\log_{10}(\mu) + 7.78\ \mathrm{dB} \quad (16)$$

where we assumed that the multi-tone signal is a sum of sine waves each with amplitude A and random phase, so that by the central limit theorem $\sigma = A\sqrt{2/N}$. The initial plan for SLEDGEHAMMER is to use the ADC designed for MUSIC [10]: 12 bits, 10.6 effective number of bits, and $f_s = 550$ MHz. If we include the averaging due to the flux ramp modulation

$$\mathrm{SNR}_{10.6} = 10\log_{10}\left(\frac{f_s}{2\times \mathrm{BW}}\right) - 10\log_{10}(N) + 58.3\ \mathrm{dB}. \quad (17)$$

For SLEDGEHAMMER, we will target a 50 kHz flux ramp rate, which gives a SNR = 72 dB for 256 channels.

In order to understand how the quantization noise limits SLEDGEHAMMER, we wish to compare it to the readout noise of the μMUX. We showed previously that the readout noise is similar to the noise temperature of the HEMT, so it is sufficient to compare the quantization noise to the voltage noise of the HEMT. The voltage on the feed line at the optimum readout power is [8]

$$V_{in} = \frac{p\Phi_0\omega_0}{4\sqrt{\eta}}\sqrt{\frac{2Z_0}{\omega_0 L_s}\frac{\lambda}{1-\lambda^2}}. \quad (18)$$

Making the same assumptions used in referring the HEMT noise to the current noise, the optimum voltage on the feed line at the input of the HEMT is 14 μV. For a HEMT noise temperature of 3 K, and a bandwidth of 350 kHz, the HEMT noise-limited SNR is 65 dB. This is likely an upper estimate since this signal to noise would be decreased by the flux ramp penalty and any masking of the transient at the flux ramp reset. Therefore, the ADC will not limit the SNR at $N = 256$ where the SNR limit due to the ADC is 72 dB, provided that the relevant signal gain is set near the optimum value. Additionally, this analysis suggests that it could be advantageous to move to an ADC with a higher sampling rate and a lower number of bits. For example, there are ADC chips available with $f_s = 3.6$ GHz and 9 effective number of bits that would also give a SNR due to the ADC of 72 dB at $N = 256$. Although there is no improvement in SNR, the over 6 times improvement in bandwidth gives much more room to place the 256 resonators or allow for more resonators on a single ADC. The increased bandwidth would allow the full 512 resonators that are planed for the final SLEDGEHAMMER instrument to be spaced 7 MHz apart and fit on a single ADC with an SNR of 69 dB.

IV. Conclusion

Microwave SQUID multiplexing has the potential to read out arrays of tens of thousands to millions of TES microcalorimeters. It has currently reached a level of maturity where it is appropriate to integrate with TESs to start to understand the limits of the technology and what components need to be improved to fulfill this potential. The 256 TES microcalorimeters planned for the initial SLEDGEHAMMER instrument are modest, but will equal the number of microcalorimeters in the largest array of TES microcalorimeters that is currently capable of simultaneous readout. SLEDGEHAMMER is designed to be a flexible test bed and a pathfinder instrument for significantly larger arrays to follow.

References

[1] D. Bennett *et al.*, "A high resolution gamma-ray spectrometer based on superconducting microcalorimeters," *Rev. Sci. Instrum.*, vol. 83, no. 9, 2012, Art. ID. 093113.

[2] A. S. Hoover *et al.*, "Determination of plutonium isotopic content by microcalorimeter gamma-ray spectroscopy," *IEEE Trans. Nucl. Sci.*, vol. 60, no. 2, pp. 681–688, Apr. 2013.

[3] W. Holland *et al.*, "SCUBA-2: the 10 000 pixel bolometer camera on the James Clerk Maxwell Telescope," *Monthly Notices Royal Astron. Soc.*, vol. 430, no. 4, pp. 2513–2533, Apr. 2013.

[4] K. Irwin, "SQUID multiplexers for transition-edge sensors," *Phys. C: Supercond.*, vol. 368, no. 1, pp. 203–210, Mar. 2002.

[5] J. Mates, G. Hilton, K. Irwin, L. Vale, and K. Lehnert, "Demonstration of a multiplexer of dissipationless superconducting quantum interference devices," *Appl. Phys. Lett.*, vol. 92, no. 2, 2008, Art. ID. 023514.

[6] O. Noroozian *et al.*, "High-resolution gamma-ray spectroscopy with a microwave-multiplexed transition-edge sensor array," *Appl. Phys. Lett.*, vol. 103, no. 20, 2013, Art. ID. 202602.

[7] K. D. Irwin and K. W. Lehnert, "Microwave SQUID multiplexer," *Appl. Phys. Lett.*, vol. 85, no. 11, pp. 2107–2109, 2004.

[8] J. A. B. Mates, "The microwave SQUID multiplexer," Ph.D. dissertation, Univ. Colorado, Boulder, CO, USA, 2011.

[9] J. Mates *et al.*, "Flux-ramp modulation for SQUID multiplexing," *J. Temperature Phys.*, vol. 167, no. 5/6, pp. 707–712, 2012.

[10] R. Duan *et al.*, "An open-source readout for MKIDs," in *Proc. SPIE Astron. Telesc.+ Instrum.*, Bellingham, WA, USA: International Society for Optics and Photonics, 2010, pp. 77 411V.

[11] S. R. Golwala *et al.*, "Status of MUSIC, the Multiwavelength Sub/Millimeter Inductance Camera," in *Proc. SPIE*, 2012, vol. 8452, Art. ID. 845 205, [Online]. Available: http://dx.doi.org/10.1117/12.926055

[12] S. McHugh *et al.*, "A readout for large arrays of microwave kinetic inductance detectors," *Rev. Sci. Instrum.*, vol. 83, no. 4, 2012, Art. ID. 044702.

[13] Collaboration for Astronomy Signal Processing and Electronics Research, http://casper.berkeley.edu

[14] W. R. Bennett, "Spectra of quantized signals," *Bell Syst. Tech. J.*, vol. 27, no. 3, pp. 446–472, Jul. 1948.

[15] W. Kester, "Taking the mystery out of the infamous formula 'SNR $= 6.02\,\mathrm{n} + 1.76$ dB' and why you should care," Analog Devices, MT-001, 2005.

[16] R. Blevins, "Probability density of finite Fourier series with random phases," *J. Sound Vibration*, vol. 208, no. 4, pp. 617–652, Dec. 1997.

[17] D. J. Mestdagh, P. Spruyt, and B. Biran, "Analysis of clipping effect in DMT-based ADSL systems," in *Proc. IEEE ICC, SUPERCOMM/ICC*, 1994, pp. 293–300.